Probing field-induced submolecular motions in a ferroelectric liquid crystal mixture with time-resolved two-dimensional infrared spectroscopy

2006 J. Phys.: Condens. Matter 18 7593

(http://iopscience.iop.org/0953-8984/18/32/008)

INSTITUTE OF PHYSICS PUBLISHING JOURNAL OF PHYSICS: CONDENSED MATTER

J. Phys.: Condens. Matter **18** (2006) 7593–7603 doi:10.1088/0953-8984/18/32/008

Probing field-induced submolecular motions in a ferroelectric liquid crystal mixture with time-resolved two-dimensional infrared spectroscopy

Jung Y Huang and Wen-Tse Shih

Department of Photonics and Institute of Electro-Optical Engineering, Chiao Tung University, Hsinchu 305, Taiwan, Republic of China

E-mail: jyhuang@faculty.nctu.edu.tw

Received 24 February 2006, in final form 11 June 2006
Published 25 July 2006
Online at stacks.iop.org/JPhysCM/18/7593

Abstract

Time-resolved two-dimensional infrared (2D IR) spectroscopy has been applied to analyse an electro-optic switching ferroelectric liquid crystal (FLC) mixture. The 2D IR correlation technique clearly shows that the Goldstone mode in the SmC* phase is suppressed by an applied electric field. The field-induced reorientation process initiates from intramolecular motions in about 10 μs. The intramolecular motions then propagate from the molecular segments attached to the same molecule to those fragments on other surrounding molecules. During the field-induced switching, the IR dipoles undergo a collective reorientation but with hindered rotation about the molecular long axis.

(Some figures in this article are in colour only in the electronic version)

1. Introduction

Ferroelectric liquid crystal (FLC) flat panel displays can provide advantages of fast response, bistability and wide viewing angle [1, 2]. However, the design of new FLC materials often proves frustrating, with the need to obtain a material with both a chiral structure and a smectic C* phase (SmC*). Although the former is achievable by synthesis, the latter is often a matter of luck. For a practical application, it further requires a wide thermodynamically stable SmC* phase. To broaden the temperature range of stable SmC* phases a eutectic by mixing several LC components can be utilized. By using this method the design of new FLC components is rendered into the doping of chiral compounds into a mixture with a wide thermodynamically stable SmC phase [3]. This approach gains significance in view that all commercial LC materials used in LC industry are mixtures.

Due to the interests of both fundamental and applied research, many efforts have been made to investigate the switching behaviour of FLC material [4–6]. It was noted that upon the reversal of the sign of an applied field, all the FLC molecules switch by rotation about a tilt

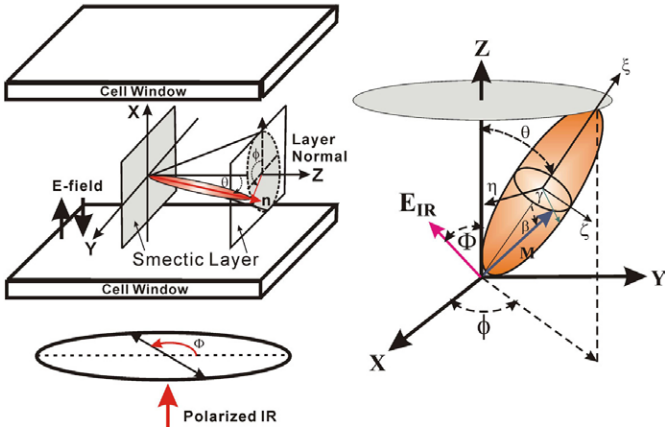

Figure 1. Schematic diagram showing the geometry of the SSFLC cell for the time-resolved infrared measurements. Z denotes the rubbing direction, which is also the layer normal of the smectic layers. **E** is the direction of the applied electric field. The incident IR polarization angle is taken as zero when its polarization direction coincides with the rubbing direction. M on the right diagram denotes the IR dipole, which tilts from the molecular long axis ξ by an angle of β and rotates about the ξ-axis by γ.

cone. This is because coupling with the applied field is through spontaneous polarization, not through coupling with any individual molecular dipoles. During the past decades, polarized Fourier transform infrared (FTIR) absorption spectroscopy has been applied to study the FLC molecular conformation during the field-induced collective reorientation process [7–10]. One of the controversial issues in this study is whether all the molecules in the ferroelectric phase switch in a rigid or flexible way. This issue becomes even more complicated for an FLC mixture. In this study, by using 2D correlation analysis of time-resolved Fourier transform infrared (trFTIR) absorption spectroscopy, interesting results about the correlated intra- and inter-molecular motions during the switching process of a surface stabilized FLC (SSFLC) mixture were obtained. Both the 2D homo-correlation and the 2D hetero-correlation are employed to deduce the detailed switching behaviours of molecular fragments.

This paper is organized as follows. In section 2, the experimental details of this study are presented. We provide a brief theoretical introduction of the 2D IR correlation technique in section 3. Experimental results and discussion are given in section 4 and finally a conclusion is drawn.

2. Experimental procedures

The SSFLC cells used consist of two CaF_2 plates coated with indium tin oxide (ITO) and polyimide alignment layers, which were rubbed unidirectionally along the Z-axis as depicted in figure 1. The substrates were separated by 1.5 μm thick spacers to meet the half-wave thickness $d_{\lambda/2} = \lambda/2\Delta n \simeq 1.9$ μm calculated with $\Delta n \simeq 0.17$ and $\lambda = 0.633$ μm. A Felix 017/100 FLC mixture (Clariant, Frankfurt, Germany) with a phase sequence of

$$\mathrm{Cr} \underset{-28\,^{\circ}\mathrm{C}}{\leftrightarrow} \mathrm{SmC}^{*} \underset{73\,^{\circ}\mathrm{C}}{\leftrightarrow} \mathrm{SmA}^{*} \underset{77\,^{\circ}\mathrm{C}}{\leftrightarrow} N^{*} \underset{85\,^{\circ}\mathrm{C}}{\leftrightarrow} \mathrm{Iso}$$

was used in view of its potential in device applications. The pretilt angle is controlled to be about 2° to allow only C1 structure to be formed. A test cell was filled with the FLC material at the temperature of the isotropic phase and then the cell was cooled slowly to 35 °C. All our SSFLC test cells exhibit a single domain examined with a polarizing microscope.

Figure 1 presents a schematic diagram of an SSFLC cell in an infrared absorption spectrometer. Time-resolved FTIR spectra from 900 to 3500 cm^{-1} with 4 cm^{-1} resolution were recorded with a liquid-nitrogen-cooled HgCdTe detector and home-made data acquisition electronics [11]. Bipolar square-wave pulses were used to excite the SSFLC cell. The waveform is comprised of a +10 V duration extending from 0 to 140 μs, followed by a field-free period from 140 to 500 μs. Then a −10 V pulse extends from 500 to 640 μs, followed by a field-free period from 640 to 1000 μs. For each polarization direction of the incident infrared radiation, a total of 32 time-resolved interferograms were acquired. The 2D correlation analysis with varying infrared polarization angles was calculated based upon an algorithm developed by Noda [12], and was implemented in 2Dshige software by Morita [13].

3. Theoretical considerations

3.1. Angular pattern of polarization-angle-dependent IR absorption peak

By using a normally incident infrared beam with a polarization at an angle of Φ relative to the rubbing direction, the absorbance pattern $A(\Phi)$ of an IR active mode can be expressed as

$$A(\Phi) = A_0 + U \cdot \cos^2(\Phi - \Phi_0), \tag{1}$$

where Φ_0 represents the apparent angle of the maximum IR absorbance. Notice that A_0 can be changed by the inclination angle β of the IR dipole moment and the fraction of isotropic component in the film. When an IR dipole freely rotates about the molecular long axis ξ, the resulting IR absorption pattern can become angular independent at a magic angle of $\beta = 54.7°$. For the case of SmC* with hindered rotation, the optical properties of the film become biaxial. The relative magnitudes of A_0 and U for all observed IR peaks can be used to deduce the underlying orientational distribution of FLC molecules.

3.2. A brief overview of the 2D IR correlation technique

Generalized two-dimensional infrared (2D IR) spectroscopy [12] is an effective mathematical tool to elucidate spectral details of a dynamic system [14]. Generalized 2D correlation is generally presented through synchronous and asynchronous plots, where synchronous 2D spectra yield very useful information about the inter- or intramolecular interactions existing in the system of interest, while asynchronous spectra are powerful for revealing the anti-correlated variation between the bands.

To construct a 2D correlation plot, we first calculate the dynamic spectra [14]

$$\tilde{I}(\nu; \alpha, t) = I(\nu; \alpha, t) - \bar{I}(\nu, t) \tag{2}$$

from a set of time-resolved IR absorption spectra $I(\nu; \alpha, t)$ perturbed by parameter α. Here t denotes the time delay. The reference spectrum $\bar{I}(\nu, t)$ can be conveniently obtained with

$$\bar{I}(\nu, t) = \frac{1}{2\pi} \int_0^{2\pi} I(\nu; \alpha, t)\, \mathrm{d}\alpha. \tag{3}$$

The synchronous $\Psi_s(\nu_1, t_1; \nu_2, t_2)$ and asynchronous $\Psi_a(\nu_1, t_1; \nu_2, t_2)$ correlation maps can then be generated from the dynamic spectra by

$$\begin{aligned} \tilde{\Psi}(\nu_1, t_1; \nu_2, t_2) &= \langle \tilde{I}(\nu_1; \alpha, t_1) \tilde{I}(\nu_2; \alpha, t_2) \rangle_{0 \leqslant \alpha \leqslant 2\pi} \\ &= \Psi_s(\nu_1, t_1; \nu_2, t_2) + \mathrm{i}\Psi_a(\nu_1, t_1; \nu_2, t_2). \end{aligned} \tag{4}$$

The bracket $\langle\ \rangle_\alpha$ denotes the correlation operation, which is defined as

$$\langle \tilde{I}(\nu_1;\alpha,t_1)\tilde{I}(\nu_2;\alpha,t_2)\rangle_{0\leqslant\alpha\leqslant 2\pi} = \frac{1}{2\pi}\int_0^{2\pi} \tilde{I}(\nu_1;\omega,t_1)\tilde{I}^*(\nu_2;\omega,t_2)\,\mathrm{d}\omega$$
$$\text{with} \qquad \tilde{I}(\nu;\omega,t) = \int_0^{2\pi} \tilde{I}(\nu;\alpha,t)\mathrm{e}^{-\mathrm{i}\alpha\omega}\,\mathrm{d}\alpha. \tag{5}$$

3.3. Probing conformation change of a molecule with 2D IR correlation technique

The generalized correlation technique allows spectra to be spread over two frequency dimensions. As a result, an enhanced spectral resolution can be obtained. However, we should note that frequency shifts and changes in bandwidth can also generate asynchronism [15] and should be taken into account when calculating and analysing 2D correlation maps. In this respect, the use of simulations is helpful for a better understanding of the experimental 2D correlation maps.

Here we summarize our previous simulation studies on 2D correlation maps: by using a set of IR spectra described by equation (1) with varying magnitudes of A_0 and U, we first discovered that the auto-peak $\Psi_s(\nu_1,\nu_1;t)$ and cross-peak $\Psi_s(\nu_1,\nu_2;t)$ of synchronous correlation are independent of A_0. But the synchronous correlation maps can vary with U by $\Psi_s(\nu_1,\nu_1;t) = 0.132\,U(\nu_1)^2$ and $\Psi_s(\nu_1,\nu_2;t) = 0.132\,U(\nu_1)U(\nu_2)$. Therefore, by using $U(\nu_1)$ as a reference, $\Psi_s(\nu_1,\nu_2;t)$ becomes a linear function of $U(\nu_2)$, suggesting that the synchronous cross-peak height may be useful to reveal the degree of molecular alignment U.

The orientation changes of molecular fragments can be revealed with a variation of Φ_0. In this regard, our simulation indicates that $\Psi_s(\nu_1,\nu_1;t)$ is insensitive to the variation of Φ_0. But the synchronous and asynchronous cross-peak heights can change with Φ_0 by $\Psi_s(\nu_1,\nu_2;t) = 0.132\cos 2[\Phi_0(\nu_1) - \Phi_0(\nu_2)]$ and $\Psi_a(\nu_1,\nu_2;t) = 0.11\sin 2[(\Phi_0(\nu_1) - \Phi_0(\nu_2)]$. Therefore, we can combine $\Psi_s(\nu_1,\nu_2;t)$ and $\Psi_a(\nu_1,\nu_2;t)$ to unveil the information about the orientation changes of molecular fragments in a complex material.

The generalized correlation approach does not require all the data to originate from within a single data set. Therefore it is possible to use the technique to compare experimental data with a variety of reference curves. For the spectra acquired at different t, we can use the hetero-correlation technique to deduce the synchronous auto-peak $\Psi_s(\nu_1,t_1;\nu_1,t_2)$, whose magnitude can be affected by both U and Φ_0 of the specific ν_1 mode. The hetero asynchronous auto-peak, however, varies only with the fragment orientation Φ_0 by $\Psi_a(\nu_1,t_1;\nu_1,t_2) = 0.11\sin[2(\Phi_0(\nu_1,t_1) - \Phi_0(\nu_1,t_2))]$. Therefore, $\Psi_a(\nu_1,t_1;\nu_1,t_2)$ is more appropriate to be used to reflect the orientation change of the molecular fragment occurring between t_1 and t_2.

We shall emphasize that in this study *the 2D asynchronous correlation analysis is used to yield information about the relative orientation changes between molecular fragments at a given time slice, while the asynchronous hetero-correlation is used to reveal the transient reorientations of molecular fragments from their corresponding directions in the field-free virgin state*. Therefore, by combining these two pieces of information together, the correlated motions of molecular fragments in a FLC material can be discovered.

4. Results and discussion

4.1. Assignment of infrared absorption bands

Figure 2(a) exhibits an infrared absorption spectrum of FELIX 017/100. Notice that the observed spectral response of an FLC mixture can be viewed to originate from an imaginary molecule with a response averaged over various species of the mixture. From this viewpoint, the

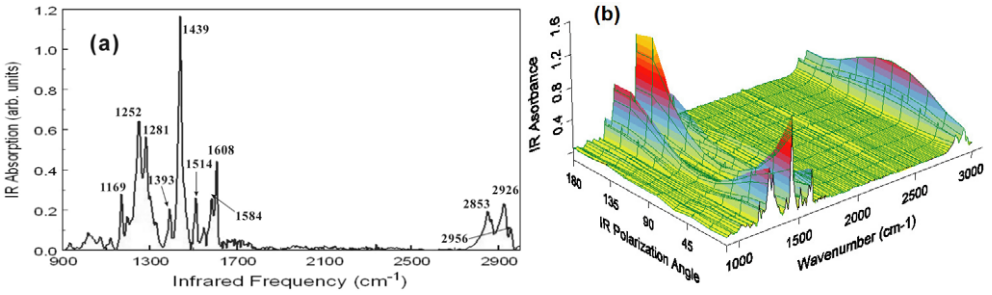

Figure 2. (a) Infrared absorption spectrum of an SSFLC cell of FELIX 017/100 in SmC* at 35 °C. (b) A set of polarized IR spectra for the SSFLC cell at 35 °C and zero field for IR polarization angle Φ in the range 0°–180°.

IR spectral peaks at 1169, 1252, 1281, 1393, 1439, 1514, 1584 and 1608 cm^{-1} can be attributed to the normal modes associated with the cores of the imaginary molecule, and the peaks at 2853, 2926 and 2956 cm^{-1} to the alkyl chains. The highest-frequency peak at 2956 cm^{-1} is noted to originate from the anti-symmetric CH_3 stretching mode, whereas the two other peaks at 2853 and 2926 cm^{-1} are from the symmetric and anti-symmetric CH_2 stretching along the alkyl chains. The peaks at 1608, 1584, 1547, 1514 and 1393 cm^{-1} are mainly from the C=C stretching modes of the benzene ring and the 1439 cm^{-1} peak could arise from the C=C stretch of the pyrimidine ring. The remaining normal modes at 1169 and 1254 (anti-sym) and 1281 cm^{-1} (sym) are associated with the C–O–C stretching modes [16]. In figure 2(b), the spectral peaks associated with the FLC cores are found to exhibit an angular dependence on the infrared polarization opposite to those of alkyl chains, reflecting the orientational-averaged IR dipole moments of cores and alkyl chains being mutually perpendicular. A similar result had also been observed with neat FLC materials [17].

4.2. Time-resolved polarized FTIR spectra

Time-resolved polarization-dependent FTIR spectra of the electro-optical switching SSFLC had been successfully acquired and used to deduce the time-resolved polarization-angle-dependent patterns for all observed IR peaks. The angular patterns allow us to determine the apparent angles Φ_0 of the IR dipoles and the corresponding dichroic ratios [18]. The results are presented in figure 3.

In viewing that the observed spectral features originate from a FLC mixture, it is surprising to discover that all apparent angles of the IR dipoles associated with the FLC cores follow nearly the same time course with a response time of $\tau_{10-90} = 45\ \mu s$. The time constant is shorter than the electro-optical response time $\tau_{10-90} = 112\ \mu s$ (see the dashed curve of figure 3(a)). The electro-optical response time can be estimated with $\tau = \gamma / P_s E$, with γ denoting the rotational viscosity, P_s the spontaneous polarization of FLC and E the applied electric field. By using the available material data of FELIX 017/100, $\gamma = 8 \times 10^{-6}$ N s cm^{-2}, $P_s = 10.5$ nC cm^{-2}, and an applied field strength of $E = 6.7 \times 10^4$ V cm^{-1}, we calculate $\tau = 114\ \mu s$, which agrees very well with the observed electro-optical response time. Since the director is inseparably coupled to the spontaneous polarization, there will be a collective reorientation of all the molecular species according to the field direction. However, the response of submolecular fragments to the applied field will be faster than the electro-optical response time, which is an averaged value over all molecular species.

The dichroic ratio of the C=C stretching mode at 1608 cm^{-1}, which is normalized to the initial value at $t = 0\ \mu s$, reaches a peak at $t = 70\ \mu s$ after the rising edge of the positive driving

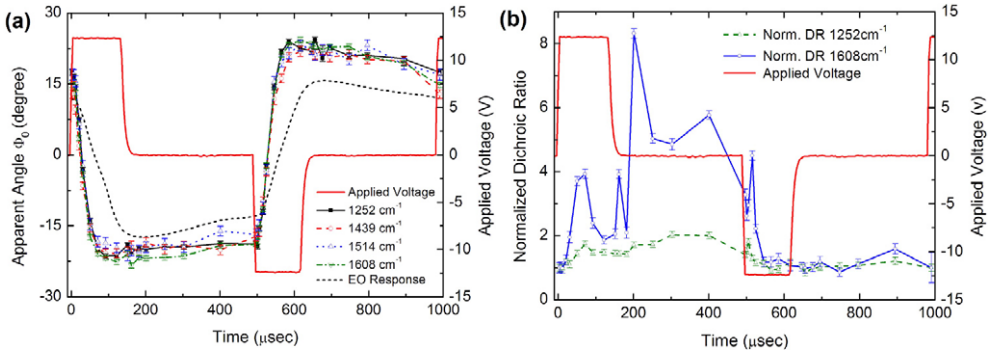

Figure 3. (a) The dynamic variation curve of the electro-optical response (dashed curve) and the averaged apparent angles of IR dipoles associated with the cores (symbols); (b) the time courses of the dichroic ratios of the C=C stretch mode at 1608 cm^{-1} normalized to the value at $t = 0$ μs (filled symbols) and C–O–C stretch at 1252 cm^{-1} (open symbols). The waveform of the bipolar driving pulses is included for reference.

field (see figure 3(b)). Significant variations were also observed near the transition edge of the applied field. The C–O–C stretching mode at 1252 cm^{-1} exhibits similar but less distinctive variation. Although the variations of IR dichroic ratio with dc voltage had also been observed on a neat FLC material [19], our result shows that the variations of dichroic ratio not only occur during the voltage-holding period but also in the field-free period. Considering that each observed IR peak can originate from molecular fragments belonging to different species, our result suggests that the C=C fragments of different species of the mixture will undergo mutual movement during the field-induced reorientation process. Since the apparent angle reflects only the averaged direction with maximum absorbance projected onto the cell substrates, it cannot exhibit the detailed variation of orientational distribution as shown in figure 3(b).

Figure 4 presents a comparison of the IR dichroic ratio (open symbols) and the corresponding synchronous auto-peak height $\Psi_s(\nu_1, \nu_1; t)$ (filled symbols) of the C=C stretching mode at 1608 cm^{-1} and the C–O–C motion at 1252 cm^{-1} associated with the FLC cores. A good correlation was observed and supports our theoretical analysis summarized in section 3.3. The time course of the synchronous auto-peak at 1608 cm^{-1} exhibits a peak at 70 μs after the rising edge of the positive pulse. At this instant, the apparent angles of all the core groups reach their extreme values (see figure 3(a)). The second maximum of the synchronous auto-peak occurs at 170 μs, where the electro-optical response of the SSFLC reaches its extreme value. We also observed significant variations in both the dichroic ratio and the synchronous auto-peak near 500 μs, where the negative field is just switched on. We do observe some differences between the dichroic ratio and the synchronous auto-peak. The deviations can originate from the influence of A_0, which has an effect on the dichroic ratio but cannot affect the synchronous auto-peak height.

4.3. 2D IR correlation analysis of the FLC mixture in steady state

The polarized IR spectra in steady states were analysed with the 2D correlation technique and are presented in figure 5. The left column of figure 5 shows the 2D synchronous correlation maps $\Psi_s(\nu_1, \nu_2)$ in the 1500–1620 cm^{-1} region, from the FLC mixture without an applied electric field (figure 5(a)), and with +5 V (figure 5(c)), −5 V (figure 5(e)) electric field. Note that three major auto-peaks are formed at 1514, 1584 and 1608 cm^{-1}, which correspond to the

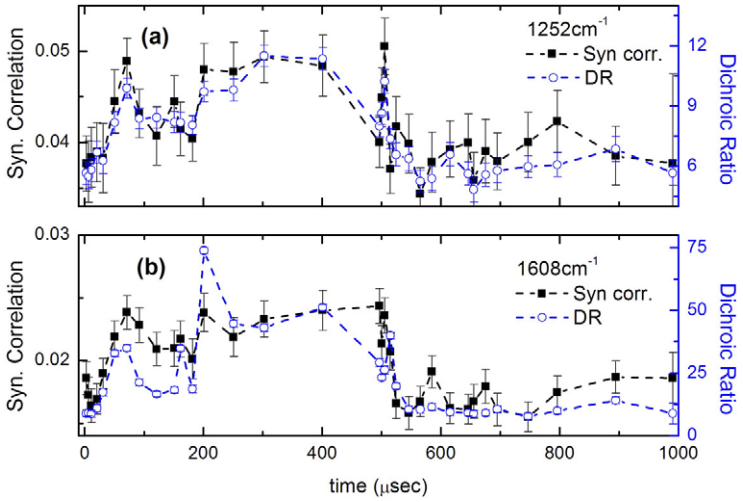

Figure 4. Comparison of the dichroic ratios (DR, open symbols) and the 2D IR synchronous auto peak (filled symbols) of (a) C–O–C stretch at 1252 cm^{-1} and (b) C=C stretch mode at 1608 cm^{-1}.

C=C stretching modes with the IR dipole moments along with that of the benzene ring. These peaks also yield significant cross-peaks, indicating a strong correlation existing among these IR active modes.

As pointed out above the asynchronous cross-peaks $\Psi_a(\nu_1, \nu_2)$ can reflect the relative orientation differences of IR dipoles. The asynchronous correlation plots $\Psi_a(\nu_1, \nu_2)$ without an applied field (figure 5(b)), with +5 V (figure 5(d)), and −5 V (figure 5(f)) are presented on the right column. The asynchronous cross-peaks are distinctive without an applied field, indicating significant Φ_0 variation existing among these C=C stretching modes. The asynchronous cross-peaks become much less distinctive when an electric field is applied. This result can be understood by noting that in the field-induced SmC* phase with unwound structure the thermal fluctuations in the azimuthal angle ϕ of the director about a tilt cone (i.e. the Goldstone mode) can be suppressed by an applied electric field and the molecular tilt plane is forced to lie on the cell substrates [20, 21]. This configuration, which corresponds to either $\phi = 90°$ or $-90°$ (see figure 1) for all the molecules depending on the field polarity, effectively reduces the angular spread of ϕ angle and therefore decreases the Φ_0 variation among the C=C stretching modes.

4.4. Time-resolved 2D IR correlation analysis of the switching dynamics of the FLC mixture

The relative orientational motions among the IR dipoles of the SSFLC mixture can be analysed by using the 2D asynchronous correlation technique. The time courses of the asynchronous cross-peaks of the C=C stretching modes, relative to the one at 1608 cm^{-1}, are presented in figure 6. These modes were chosen to properly reflect the major C=C stretching motions based on their synchronous and asynchronous cross-peak heights. It is interesting to note that the cross-peaks of all other C=C stretching modes are higher than the 1608 cm^{-1} mode from 0 to 500 μs and become lower during the negative-voltage driving cycle. Based on our simulation, we conclude that all the C=C stretching modes relative to the 1608 cm^{-1} mode are rotated on the SmC* cone with a smaller Φ_0 during the positive-voltage driving cycle and with a larger Φ_0 during the negative-driving cycle. This implies that during the field-induced switching

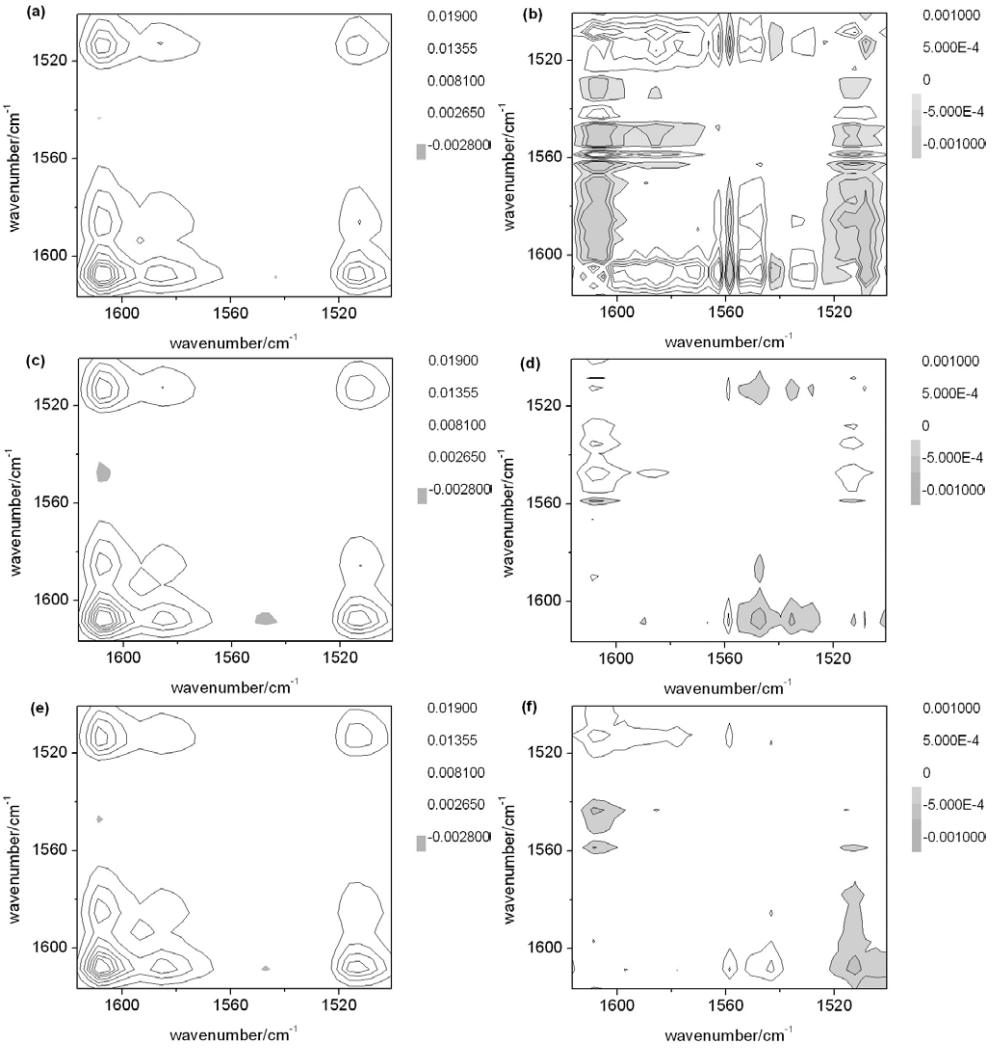

Figure 5. (Left column: (a), (c), (e)) Synchronous 2D IR correlation plots $\Psi_s(\nu_1, \nu_2)$ in the 1620–1500 cm^{-1} region generated from the polarization-angle-dependent (from 0° to 180°) spectral variations of FELIX 017/100 in SmC* at 35 °C (a) without an external field, (c) applying DC +5 V and (e) −5 V; (right column: (b), (d), (f)) the corresponding 2D IR asynchronous correlation plots $\Psi_a(\nu_1, \nu_2)$ in the 1620–1500 cm^{-1} region.

the effective FLC molecules will rotate about the layer normal with hindered rotation about the molecular long axis. The speed of this restricted rotation is slower than that of the field-induced rotation about the layer normal.

The switching dynamics can be better understood by monitoring the field-induced reorientation of different molecular fragments by using the 2D hetero-correlation technique. However, we shall emphasize that the asynchronous peak height is changed not only with the orientation of the IR dipole but also with the spectral intensity of the IR absorption peak. To remove the influence of the spectral intensity variations among different IR active modes and retrieve correctly the orientational variation, a global 2D phase map is more

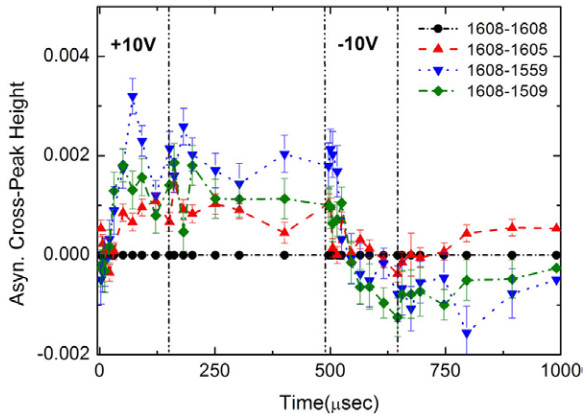

Figure 6. Dynamic variations of the 2D IR asynchronous correlation of C=C stretching modes with respect to the C=C stretching mode at 1608 cm^{-1}.

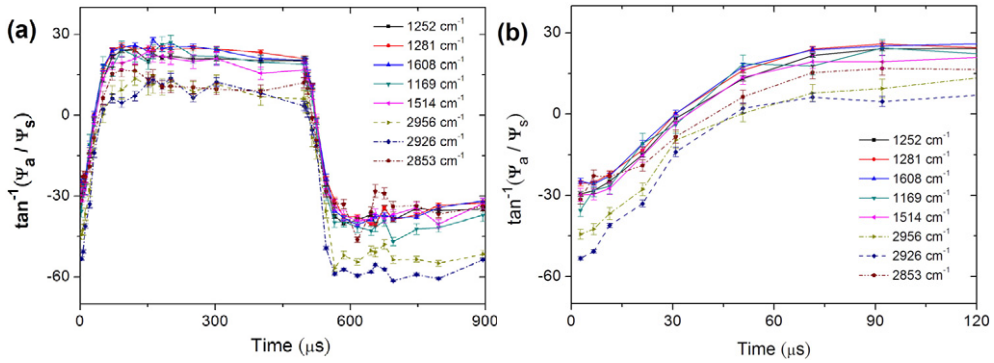

Figure 7. (a) Time courses of 2D IR hetero-correlation phase angles calculated from the time-resolved polarization-angle-dependent spectra of FELIX 017/100 at 35 °C; (b) the expanded view of (a) near the rising edge of the positive driving pulse.

appropriate [14]. The global phase map can be obtained by calculating the arctangent of $\Psi_a(\nu_1, t; \nu_1, 0)/\Psi_s(\nu_1, t; \nu_1, 0)$.

The time courses of 2D IR hetero-correlation phase angles are shown in figure 7(a). The phase angles of the molecular segments were found to change signs during the field driving cycles, clearly indicating that the field-induced reorientations of the molecular segments point to the two opposite sides of their corresponding field-free virgin directions. We also found that all the core segments are closely tied together even though they may be attached to different species. Those stretching modes associated with the alkyl chains are connected more flexibly to yield a larger angular deviation from the core groups. An expanded view near to the zero point is presented in figure 7(b), which shows that the relative order and phase differences are preserved during the orientation switching. If the IR dipoles rotate freely about the molecular long axis, the relative order and 2D phase angles will be changed and their phase differences will not be preserved during the field-induced orientational switching. Thus our result shown in figure 7(b) strongly supports the notion of a collective reorientation of the molecular fragments with hindered rotation about the molecular long axis.

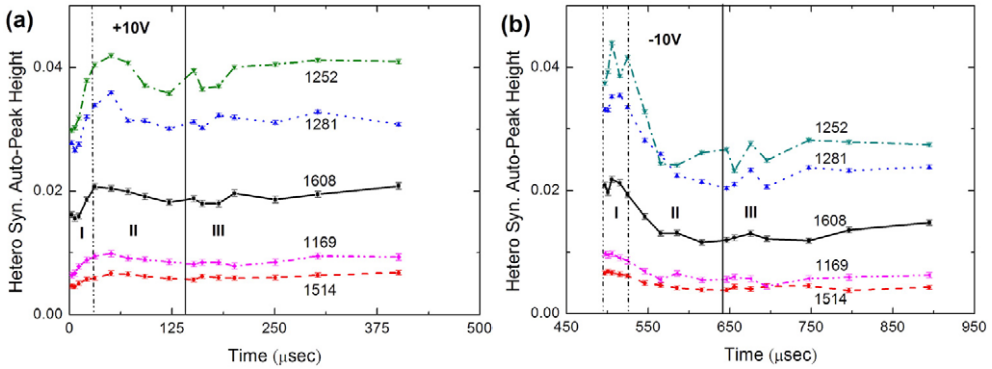

Figure 8. The time courses of 2D IR hetero-synchronous auto peaks generated from the time-resolved polarization-angle-dependent spectra from 0° to 180° of FELIX 017/100 at 35 °C during (a) the positive voltage driving cycle and (b) the negative voltage driving cycle. Stage I and II denote the field-on duration and stage III is the field-free period.

To investigate the relative motions among molecular fragments further, 2D synchronous hetero-correlation analysis of the IR spectra between the field-free virgin state and the field-induced switching states is employed. The 2D hetero-synchronous auto-peaks of the IR dipoles associated with the cores of the molecular species are presented in figure 8. We notice that the synchronous hetero-correlations of the molecular fragments are increased (therefore have a higher degree of alignment U) during the positive field-on period. During the positive driving cycle, the hetero-synchronous auto-peak at 1608 cm^{-1} exhibits a first maximum at 30 μs after the rising edge of the positive driving pulse; while the stretching modes at 1252, 1281 cm^{-1} reach their first peaks with a slightly longer delay time of 60 μs. This interesting finding can be interpreted with the more rigid nature of the C=C stretching mode at 1608 cm^{-1}, therefore exhibits a faster field-induced reorientation.

We can divide the time courses of 2D hetero-synchronous auto-peaks into three stages. In stage I, the observed variations of angular spread are rather rapid. We attribute the transient behaviour during this stage to field-induced intramolecular motions. The hetero-synchronous correlations during stage I are nearly constant at the initial 10 μs, indicating that the relative orientational motions are minor and the motions will occur among the functional groups attached to the same molecule. After 10 μs while the field is still applied, the hetero-synchronous auto-peak heights begin to increase, which suggests that the correlated motions propagate from the molecular fragments belonging to the same molecule to those on other surrounding molecules. In the stage II, the observed gradual but significant variations in the hetero-synchronous correlations could be due to the higher degrees of freedom in the field-induced intermolecular motions. The variations in the angular spreads persist even after the applied field is switched off.

5. Summary

Time-resolved infrared two-dimensional correlation (2DC) and hetero-correlation (2DHC) techniques have been applied to analyse an electro-optic switching surface-stabilized ferroelectric liquid crystal (SSFLC) mixture.

The 2DC analysis revealed that the thermal fluctuations in the azimuthal angle of the FLC director about a tilted cone in the SmC* phase are effectively suppressed by electric field. The

2DHC technique reveals a collective reorientation of the molecular fragments about an SmC* cone with hindered rotation about the molecular long axis. The restricted rotation is slower than that of the field-induced rotation about the layer normal. The field-induced molecular reorientation starts with intramolecular motions, which proceeds in about 10 μs. Then the intramolecular motions spread from the IR dipoles attached to the same molecule to those IR dipoles on other surrounding molecules.

Acknowledgments

We acknowledge the financial support from the National Science Council of the Republic of China under grant NSC 94-2112-M-009-031 and Taiwan TFTLCD Association Foundation No A623TT4000-V14.

References

[1] Clark N A and Lagerwall S T 1980 *Appl. Phys. Lett.* **36** 899
[2] Lagerwall S T 1999 *Ferroelectric and Antiferroelectric Liquid Crystals* (Weinheim: Wiley–VCH)
[3] Walba D M 1991 *Advances in the Synthesis and Reactivity of Solids* vol 1 (London: JAI Press) pp 173–235
[4] Park B *et al* 1999 *Phys. Rev.* E **59** R3815
[5] Jang W G, Park C S and Clark N A 2000 *Phys. Rev.* E **62** 5154
[6] Zhao J G, Yoshihara T, Siesler H W and Ozaki Y 2002 *Phys. Rev.* E **65** 021710
[7] Hide F, Clark N A, Nito K, Yasuda A and Walba D M 1995 *Phys. Rev. Lett.* **75** 2344
[8] Shilov S V, Skupin H, Kremer F, Wittig T and Zentel R 1997 *Phys. Rev. Lett.* **79** 1686
[9] Verma A L, Zhao B, Terauchi H and Ozaki Y 1999 *Phys. Rev.* E **59** 1868
[10] Kocot A, Wrzalik R, Orgasinska B, Perova T, Vij J K and Nguyen H T 1999 *Phys. Rev.* E **59** 551
[11] Masutani K, Sugisawa H, Yokota A, Furukawa Y and Tasumi M 1992 *Appl. Spectrosc.* **46** 560
[12] Noda I 1993 *Appl. Spectrosc.* **47** 1329
[13] Morita S 2004 2Dshige©, Kwansei-Gakuin University (http://sci-tech.ksc.kwansei.ac.jp/∼ozaki/)
[14] Ozaki Y and Noda I 2000 *Two-Dimensional Correlation Spectroscopy* (*AIP Conf. Proc.*) vol 508 (Melville, NY: AIP)
[15] Czarnecki M A 1998 *Appl. Spectrosc.* **52** 1583
[16] Zhao J G, Yoshihara T, Siesler H W and Ozaki Y 2001 *Phys. Rev.* E **64** 031704
[17] Verma A L, Zhao B, Bhattacharjee A and Ozaki Y 2001 *Phys. Rev.* E **63** 051704
[18] Shih W T, Huang J Y and Zhang J Y 2004 *Liq. Cryst.* **31** 377
[19] Sigarev A A, Vij J K, Lewis R A, Hird M and Goodby J W 2003 *Phys. Rev.* E **68** 031707
[20] Brown C V and Jones J C 1999 *Appl. Phys. Lett.* **86** 3333
[21] Vaupotic N, Grubelnik V and Copic M 2000 *Phys. Rev.* E **62** 2317